

# Deformation Processing of PMMA into High-Strength Fibers

C. A. BUCKLEY,\* E. P. LAUTENSCHLAGER, and J. L. GILBERT

Division of Biological Materials, Northwestern University, Chicago, Illinois 60611

## SYNOPSIS

Poly(methyl methacrylate) was drawn into fibers by melt extrusion followed immediately by a transient temperature drawing process. By varying five processing variables, fibers ranging from 0.635 mm to 25  $\mu\text{m}$  in diameter were produced. Heat-induced relaxation of the aligned structure was used to determine the draw ratio of the resultant fibers and therefore the degree of polymer chain alignment imposed by the deformation process. The resulting changes in length and diameter were measured and it was found that draw ratios of 5–20 had been achieved under the varying processing conditions. It was also observed that fiber diameter immediately after drawing is a good predictor of the degree of orientation present in the fiber irrespective of the processing conditions. To test the effect molecular orientation has on material properties, fibers with varying degrees of orientation were tested in tension. As expected, increasing alignment resulted in increasing tensile strength. The maximum observed true ultimate tensile strength was  $225 \pm 53$  MPa and was seen in fibers with a draw ratio equal to  $18.7 \pm 4.5$ . Fibers with a lower degree of alignment, while not as strong in tension, exhibited significantly increased ductility. True strains of as high as 25% were observed.

## INTRODUCTION

Because of its superior biocompatibility, poly(methyl methacrylate) (PMMA) is widely used in orthopedic surgery as a bone cement in total joint replacements. As the success of this procedure has improved, PMMA, being brittle and relatively low-strength, has been identified as a weak link in the system. As a result, there has been considerable effort to improve the properties of PMMA so that its fatigue behavior more closely matches that of the prostheses it fixes. Much of this effort has involved the reinforcement of PMMA with high strength fibers of stainless steel, carbon, or Kevlar.<sup>1–3</sup> The properties of these composites are controlled by the strength of the fiber–matrix bond, which for the fibers mentioned is fairly low. One alternative is to fabricate a self-reinforced composite consisting of PMMA fibers reinforcing a PMMA matrix. The resulting composite would possess a high fiber–matrix bond strength, with corresponding improvements in

mechanical properties. The first step toward producing this composite is to fabricate these PMMA fibers and completely characterize their properties.

The intent of the present study is twofold. First, we seek to determine the effects of thermal and mechanical processing conditions on the draw ratios of oriented poly(methyl methacrylate) (PMMA) fibers by producing fibers under a wide range of conditions. Draw ratios are then determined using a heat relaxation method. Second, the mechanical properties of the fibers resulting from the various processing conditions are determined. The relationships between the amount of orientation in the fibers, as measured by heat-induced relaxation, and the mechanical properties of ultimate tensile strength, strain to failure, and Young's modulus are presented and related to molecular structure of the oriented polymer.

## MATERIALS AND METHODS

### Extrusion and Drawing

Using the apparatus schematically pictured in Figure 1, PMMA fibers were extruded and drawn under various conditions in the interest of determining the

\* To whom correspondence should be addressed.

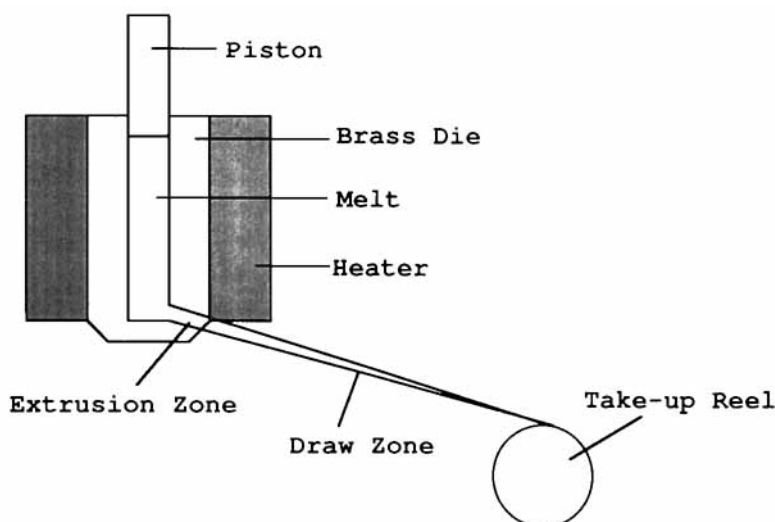


Figure 1 Drawing apparatus.

processing procedure which produces the most highly aligned, and therefore the strongest fiber. Five parameters were varied to do so: the temperature of the molten acrylic prior to extrusion and drawing, designated as  $T_m$ ; the rate at which the molten acrylic is forced toward the extrusion hole, or the extrusion velocity,  $V_e$ ; the diameter of the extrusion hole,  $d_e$ ; the rate at which the extruded fiber is taken up, or the draw velocity,  $V_d$ ; and finally, the temperature of the medium into which the fiber is drawn, or the cooling temperature,  $T_c$ .

Pieces of commercially available PMMA rod (Cadillac Plastics, Inc.) were placed in a brass die and heated to 170°C by means of an electric heater encircling the die (Buehler, Lake Bluff, IL). Melt temperature was measured with a thermocouple placed into the die through the extrusion hole prior to drawing. A brass plunger was attached to the crosshead of the Instron tensile testing machine (Instron Engineering Corp., Canton, MA) and lowered into the opening of the die. The plunger was lowered at a constant rate for the extrusion of each fiber (from 0.0254 to 1.27 cm/min) and the fiber was extruded through one of several holes at the base of the die. These holes were drilled in a 45° bevel at the end of the die and varied in diameter from 0.102 to 0.277 cm.

The entire drawing apparatus was placed on the compression load cell of the Instron mechanical test system so that plunger load could be monitored throughout the extrusion process to ensure that the molten PMMA in the die was always under pressure. The extruded fiber was either cooled in air ( $\sim 25^\circ\text{C}$ ) or quenched in an ice water bath ( $\sim 4^\circ\text{C}$ ) placed

immediately adjacent to the extrusion hole and was taken up on a variable speed drum at speeds continuously ranging from 4.31 to 30.3 m/min. In the experiments using an ice water quench, the bath was placed such that the fiber traveled less than 1 cm before being immersed in the bath. For each combination of extrusion parameters (temperature of melt, extrusion velocity, extrusion hole diameter, and quench temperature), the fiber was drawn at increasing speeds to the point at which the fiber failed.

### Heat Relaxation

From each fiber (a fiber being defined by a unique combination of the five extrusion and drawing parameters) several samples of known length (approximately 2–5 cm) and diameter were cut and placed in a furnace and heated above their glass transition temperature  $T_g$  (about 110°C) until the nonequilibrium “frozen in” molecular alignment of polymer chains began to relax to its random coil configuration, resulting in a decrease in fiber length and an increase in fiber diameter. Relaxation was considered to be complete when the bending and twisting of the fiber associated with relaxation ceased, and the fiber laid flat and straight for some time. The fibers were then removed from the heat, final lengths and diameters were measured using a micrometer, and relaxation ratios,  $\Gamma_L$  and  $\Gamma_D$ , were calculated as follows:

$$\Gamma_L = l_{\text{initial}}/l_{\text{final}}$$

$$\Gamma_D = d_{\text{final}}/d_{\text{initial}}$$

where  $l_{\text{initial}}$  = unrelaxed length and  $l_{\text{final}}$  = heat relaxed length, and  $d_{\text{initial}}$  = unrelaxed diameter and  $d_{\text{final}}$  = heat relaxed diameter.

### Fiber Tensile Tests

In order to measure the ultimate tensile strength (UTS), strain to failure, and modulus of individual fibers, the ends of a fiber sample were placed in a flame and allowed to melt to bulbs. This resulted in a gradual taper from the grip point to the fiber's gage diameter, ensuring that the fiber broke along the gage length rather than at the grip points.

The ends of the tensile samples were placed in the grips of the Instron and separated at a rate of 0.254 cm/min. True ultimate tensile strength, true strain to failure, and elastic modulus were calculated as follows:

$$\sigma = \frac{P}{A_i} \left( 1 + \frac{\Delta l}{l_i} \right)$$

$$\epsilon = \ln \left( 1 + \frac{\Delta l}{l_i} \right)$$

$$E = \sigma / \epsilon$$

where  $\sigma$  is the true stress,  $P$  is the maximum load sustained by the sample,  $A_i$  is the initial cross-sectional area of the sample,  $\Delta l$  is the change in length of the sample during testing,  $l_i$  is the initial length of the sample,  $\epsilon$  is the true strain, and  $E$  is the modulus. Tensile tests were performed on fibers of diameters varying from 0.0036 to 0.0610 cm. For comparative purposes, samples of bulk acrylic (Jet Acrylic, Lang Dental Manufacturers, Chicago, IL) were tested.

### Scanning Electron Microscopy (SEM)

SEM micrographs of fractured fiber samples were taken using a Cambridge Instruments Model S120 scanning electron microscope (Cambridge, U.K.). Prior to imaging, samples were sputter-coated with gold.

## RESULTS

### Extrusion and Drawing

Each of the five extrusion and drawing parameters exerted a unique and predictable effect on the qualities of the resultant fiber; these effects interacted in such a way that it was possible to qualitatively

predict the characteristics of a fiber produced by any given combination of parameter settings. The thickest fibers resulted from a fast extrusion speed, a large extrusion hole diameter, and a slow draw rate, whereas the finest, most highly aligned fibers were obtained with a slow extrusion speed, a small extrusion hole diameter, and a fast draw rate.

The temperature of the melt and the cooling temperature seemed to affect the surface appearance of the fiber rather than its diameter. At temperatures around 160°C, the melt was still quite viscous, and high pressures were required to force it out the extrusion hole. Once out, the acrylic would not draw at all, and fiber formation was impossible. A melt temperature of about 169°C, however, resulted in fibers that drew down to as small as 25  $\mu\text{m}$  in diameter under optimal drawing and extrusion conditions. These fibers were smooth on the surface and were relatively uniform in diameter throughout their length. When the temperature of the melt was raised to 179°C, bubbles formed in the melt and audibly popped as they reached the extrusion hole. This resulted in some surface roughness and an uneven diameter distribution along the length of the fiber.

The cooling temperature had similar but more pronounced effects on the surface quality of the finished fiber. Fibers cooled in air were smooth, even and pliant, but those pulled through an ice water bath were very rough to the touch, variant in diameter, and extremely brittle; they often broke with handling and were much more prone to breaking during drawing. As a result, drawing fibers through ice was eventually abandoned as was using a melt temperature of 179°C. All results presented here are from fibers drawn from a melt at 169°C and cooled in air.

### Heat Relaxation

When fibers were heated slowly from room temperature, it was found that relaxation began at 80–90°C, depending on fiber diameter, with the larger diameter fibers beginning to relax before those of smaller diameters. Complete relaxation occurred at temperatures well above  $T_g$ , approaching the temperature of original deformation,  $T_m$ . At the onset of relaxation, the release of stored energy in the fibers caused them to bend, twist, and curl up on themselves; when relaxation was complete, the fibers lay still and straight.

Sixty-eight different types of fibers were tested for their heat relaxation behavior. Their lengths decreased from 5–20 times during heating, while their diameters increased by factors of 2–6. The plots in

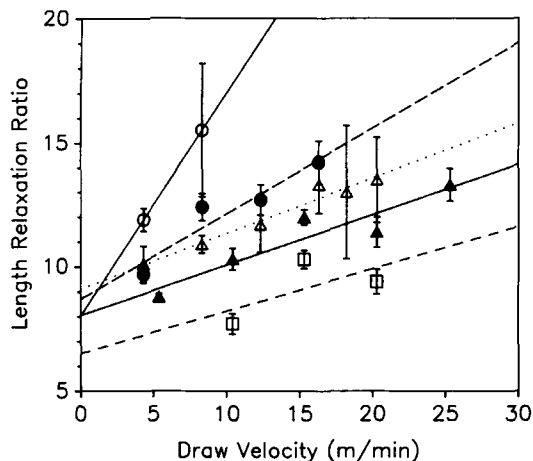


**Figure 2** Length relaxation ratio vs. draw velocity for five different extrusion velocities (cm/min): (○) 0.0254; (●) 0.127; (△) 0.254; (▲) 0.508; (□) 1.27. Fibers were drawn from a melt at 169°C, through a 0.178 cm hole, into air.

Figures 2–5 illustrate the relationship between  $\Gamma_L$  or  $\Gamma_D$ , the extrusion velocity ( $V_e$ ), and the draw velocity ( $V_d$ ) for a melt temperature of 169°C, a cooling temperature of 25°C, and extrusion hole diameters of either 0.178 or 0.102 cm. Each point on a plot represents the average of five to ten relaxation samples from a given fiber.  $R$  values for the regression lines shown in these plots are given in Table I.

As suggested above, decreasing  $V_e$  and increasing  $V_d$  leads to increasingly fine fibers with a correspondingly high degree of chain alignment as re-

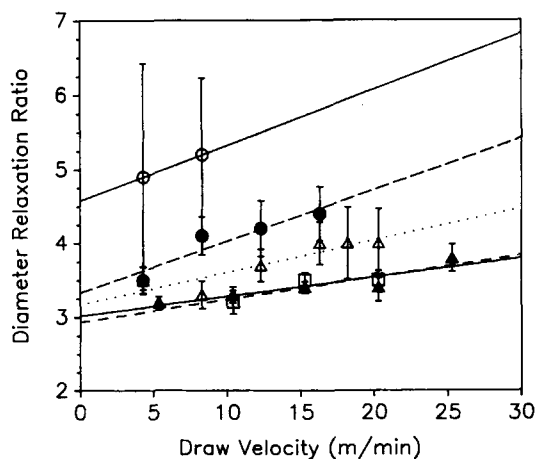


**Figure 3** Diameter relaxation ratio vs. draw velocity for five different extrusion velocities (cm/min): (○) 0.0254; (●) 0.127; (△) 0.254; (▲) 0.508; (□) 1.27. Fibers were drawn from a melt at 169°C, through a 0.178 cm hole, into air.

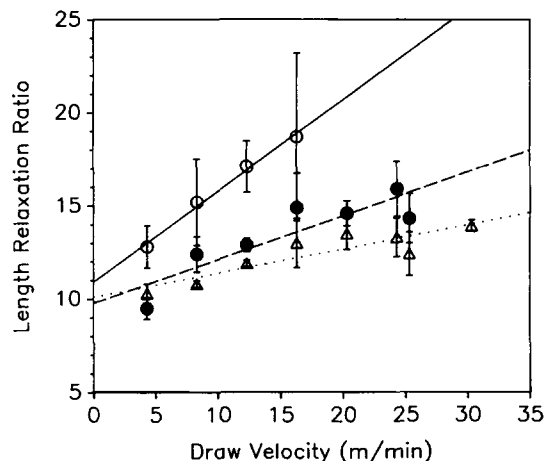


**Figure 4** Length relaxation ratio vs. draw velocity for three different extrusion velocities (cm/min): (○) 0.0254; (●) 0.127; (△) 0.254. Fibers were drawn from a melt at 169°C, through a 0.104 cm hole, into air.

flected in the relaxation ratios. Figures 2 and 3 illustrate the results for fibers drawn through the larger extrusion hole ( $d_e = 0.178$  cm). Several trends emerge: (1) increasing draw velocity increases the degree of alignment; (2) decreasing the extrusion velocity increases the degree of alignment obtained at a given draw velocity; and (3) the slopes of these lines increase with decreasing extrusion velocity. These three trends hold for both length and diameter relaxation ratios. The most highly aligned fiber produced under these conditions was that drawn at  $V_d = 8.30$  m/min and  $V_e = 0.0254$  cm/min. Its draw ratio was  $15.5 \pm 2.69$  and  $\Gamma_D = 5.2 \pm 1.03$ . As is true

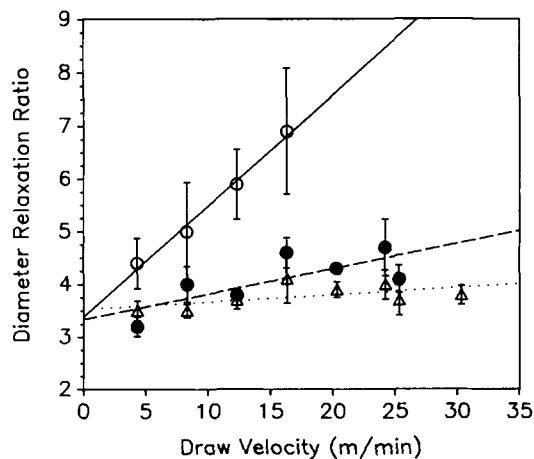


**Figure 5** Diameter relaxation ratio vs. draw velocity for three different extrusion velocities (○) 0.0254; (●) 0.127; (△) 0.254. Fibers were drawn from a melt at 169°C, through a 0.104 cm hole, into air.

**Table I** *R* Values for Regression Lines Shown in Figures 2–5

	Extrusion Velocity (cm/min)				
	0.0254	0.127	0.254	0.508	1.27
Figure 2	1.00	0.951	0.980	0.935	0.639
Figure 3	1.00	0.933	0.892	0.902	0.863
Figure 4	0.996	0.882	0.888		
Figure 5	0.994	0.751	0.564		

under many extrusion and drawing conditions used in this study, the standard deviations of the most highly oriented fibers are slightly higher than those of less highly aligned fibers.

Figures 4 and 5 depict the relaxation behavior of fibers extruded through the smaller extrusion hole ( $d_e = 0.102$  cm) and show that this drawing condition results in the most highly aligned fibers as measured by both length and diameter relaxation ratios. The fiber drawn at  $V_e = 0.0254$  cm/min and  $V_d = 16.3$  m/min decreased in length by  $18.7 \pm 4.51$  times and increased in diameter by  $6.9 \pm 1.19$  times during heat relaxation, both of which are the highest values observed for the fibers produced in this study. A draw ratio of 18.7 represents approximately a four-fold increase over the maximum draw ratio previously reported for PMMA.<sup>4</sup> The curves in Figures 4 and 5 have similar trends in slope as the corresponding curves in Figures 2 and 3, the difference being that the smaller extrusion hole allows drawing at higher draw velocities, resulting in finer fibers.

Figure 6 illustrates the relationship that emerged between a fiber's diameter after drawing and its length and diameter relaxation ratios. Each of the points on the curve represents the average shrinkage ratio of at least five samples of a fiber drawn at a unique  $V_e$ ,  $V_d$ , and  $d_e$ . All fibers represented in this plot resulted from a melt temperature of 169°C and were cooled in air. This plot suggests that, for given melt and cooling temperatures, a fiber's unrelaxed diameter is a good predictor of its relaxation behavior and presumably of its degree of chain alignment, regardless of the processing conditions which led to that diameter. For example, a fiber drawn at  $V_e = 0.254$  cm/min,  $V_d = 25.3$  m/min, and  $d_e = 0.102$  cm had an average diameter of 0.0130 cm and another drawn at  $V_e = 0.127$  cm/min,  $V_d = 8.30$  m/min, and  $d_e = 0.178$  cm had an average diameter of 0.0140 cm. Both fibers decreased in length by 12.4 times upon heating ( $\pm 1.18$  and  $\pm 0.55$ , respectively), and their diameters increased by  $3.7 \pm 0.29$  and 4.1

$\pm 0.26$  times, respectively, although their processing conditions were quite different.

### Fiber Tensile Tests

Fibers of diameters spanning the range produced in this study were tested in tension in order to observe the effects of chain alignment on tensile properties. For comparison, bulk acrylic was shown to exhibit ultimate tensile strengths of 25–30 MPa and elongations of 4–6%.

Immediately evident from tensile tests of these fibers is that their properties are much different than those of bulk acrylic, as can be seen in the stress-strain curves of representative fibers shown in Figure 7. Although the bulk sample breaks in a brittle fashion, exhibiting essentially only elastic deformation prior to failure, the fibers exhibit a distinct yield point and deform plastically. Those fibers with a lesser degree of orientation elongate much more than those with a higher degree of orientation; the fiber with relaxation ratio of 6 exhibits a strain to failure of 19.1% as opposed to the fiber with  $\Gamma_L = 13$ , which elongates by only 6.3% before failing. Although the most highly aligned, strongest fiber of the three shown in this figure has a relatively low strain to failure, it does exhibit a distinct yield point ( $\sigma_{ys} = 122$  MPa) in contrast to the bulk acrylic sample. The induction of orientation, in addition to increasing strength, dramatically increases the modulus of these fibers, as seen in Figure 7. The SEM micrographs shown in Figures 8 and 9 illustrate the ductile failure of a partially aligned fiber quite clearly.

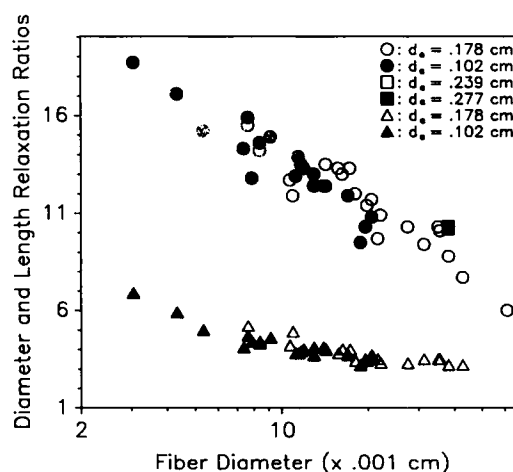


**Figure 6** Correlation between relaxation ratios and fiber diameter for fibers drawn from a melt at 169°C and cooled in air. Circles and squares are length relaxation ratios and triangles are diameter relaxation ratios.

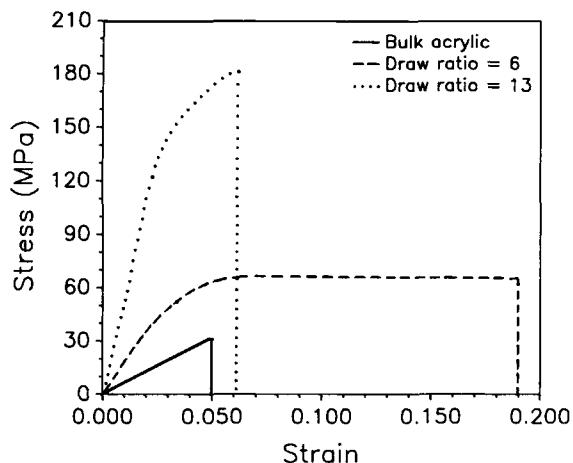


**Figure 7** Stress-strain curves for a bulk acrylic sample, a fiber with diameter 0.0102 cm,  $\Gamma_L = 13$ , UTS = 181 MPa, and true strain = 6.3%, and a fiber with diameter 0.0528 cm,  $\Gamma_L = 6$ , UTS = 63.5 MPa, and true strain = 19.1%. A modest amount of orientation results in a vastly increased strain to failure over the bulk material, whereas a greater degree of alignment results in an increased ultimate strength.

Rather than the smooth, clean break observed in the fracture of bulk acrylic, this fiber ( $d = 0.028$  cm,  $\Gamma_L = 10$ ) has stretched and frayed much like a rope. The increase in sample elongation mentioned earlier manifests itself in the very ductile fracture observed in these micrographs. The fracture of the acrylic fiber of Figure 8 (shown at greater magnification in Fig. 9) suggests a gradual failure of small bundles of aligned polymer, giving the frayed appearance, and, finally, the longitudinal splitting of the remaining fiber along the aligned direction. The fiber

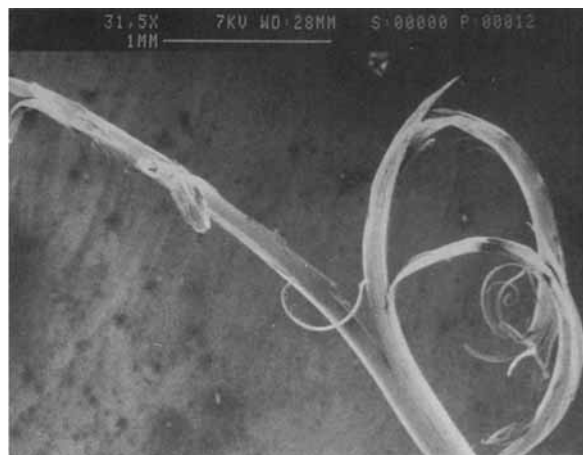


**Figure 8** SEM micrograph (32X) of a fiber tensile sample. Fiber diameter is 0.028 cm, and  $\Gamma_L = 10$ .

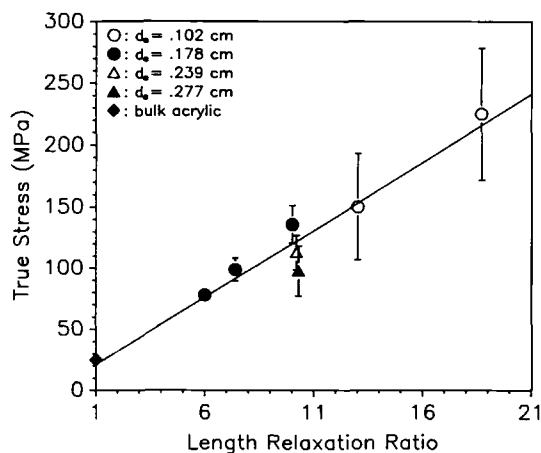


**Figure 9** Higher magnification (275X) of fiber tensile sample in Figure 8.

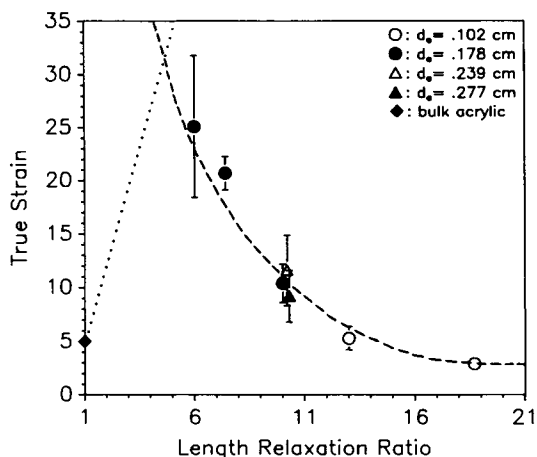
shown in these micrographs exhibited a true strain to failure of 12% in a tensile test.

Figure 10 shows the linear increase in true ultimate tensile strength with increasing length relaxation ratio. A maximum UTS of 225 MPa was observed in the fiber of 0.0036 cm diameter, whose length relaxation ratio was 18.7. This represents approximately a 600% increase in strength over the bulk material. The minimum fiber UTS, 78.0 MPa, was seen in the fiber of largest diameter (0.061 cm) and smallest length relaxation ratio (6.0) measured in this study.

Measurements of sample elongation exhibited a trend opposite to strength (Fig. 11). True strain to failure decreased exponentially with length relaxation ratio. A maximum strain to failure of 25% was observed in the fiber with  $d = 0.061$  cm and length relaxation ratio of 6.0; this is the same fiber that



**Figure 10** True stress vs. length relaxation ratio.



**Figure 11** True strain to failure vs. length relaxation ratio.

exhibited the lowest ultimate tensile strength of all of the fibers tested. The minimum elongation (2.9%) occurred in the strongest fiber ( $d = 0.0036$  cm).

Modulus was also affected by the induction of orientation as seen in Figure 12. Like true stress, modulus increases with increasing length relaxation ratio. The strongest fiber tested in tension ( $\Gamma_L = 18.7$ ) had a modulus of  $7.80 \pm 1.71$  GPa, while the least highly aligned fiber had a modulus of  $2.08 \pm 0.231$  GPa. Control samples of bulk acrylic exhibited moduli of 0.42–0.75 GPa.

## DISCUSSION

### Drawing and Heat Relaxation

It is generally believed that the induction of orientation in amorphous polymers is difficult and that orientation in glassy polymers does not occur to nearly the degree it does in crystalline polymers. This is due, in part, to the fact that, in amorphous polymers such as PMMA, the deformation required to achieve orientation causes brittle failure before a change in molecular structure can be effected. Previous investigations have reported draw ratios for PMMA up to only 4.5 at temperatures of  $135^\circ\text{C}$ .<sup>4</sup> The mechanism by which amorphous polymers become oriented is not well understood, although it has been speculated that it involves the alignment of chain bundles that exist in the undeformed "amorphous" state.<sup>5</sup> In other words, amorphous polymers are not truly amorphous but contain a basic structural unit, the chain bundle, which is capable of being aligned in response to an applied deformation.

In the present study, by elevating the temperature at which deformation started to  $169^\circ\text{C}$  and using a transient temperature drawing process, bulk poly (methyl methacrylate) was drawn into fibers of diameters as small as  $25 \mu\text{m}$ . Although direct measurement of extension ratios was prohibited by the drawing configuration, draw ratio was approximated by measurement of residual strain upon heat-induced relaxation of fibers. This method revealed draw ratios of up to 18.7, a fourfold increase over the values previously reported.

In the processing configuration used in the current work, there are three main regions of deformation: inside the die, where the melt is subject to the compressive force of the piston; at the extrusion hole, where the first significant decrease in cross-sectional area of the acrylic occurs; and, once outside the die, during the drawing phase, where further reduction in fiber cross section occurs. The results of this work suggest that it is the total amount of imposed tensile deformation, not the particular combination of processing parameters which results in this deformation, which determines the molecular structure of the resultant fiber.

It was shown that a fiber's diameter immediately after drawing is a good indicator of how much deformation the structure has undergone to reach its final state for the conditions considered (Fig. 6). Therefore, the degree of orientation (as measured by heat-induced relaxation) and the resultant mechanical properties, such as tensile strength, can be directly related to a fiber's diameter after drawing. Because chains experience tensile forces during the drawing phase, it is the deformation which occurs here that plays the most significant role in determining the degree of alignment in a fiber. With all

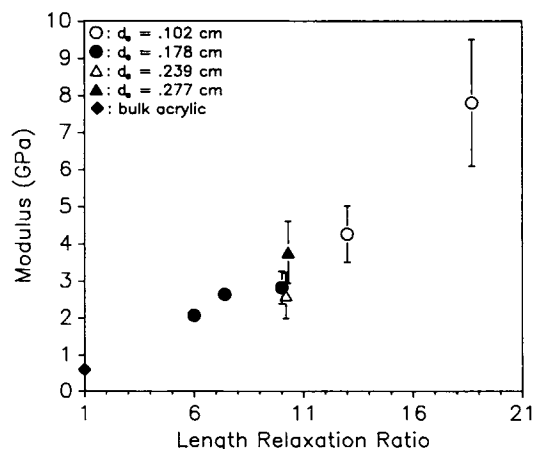


**Figure 12** Young's modulus vs. length relaxation ratio.

other parameters held constant, increasing draw rate decreases fiber diameter and increases length relaxation ratio.

The diameter of the extrusion hole does not appear to directly contribute to the degree of alignment in the final fiber but does affect the rate at which the fiber may be drawn without breaking. The smallest opening permits much higher draw rates, which allows more tensile deformation during drawing and thus results in a greater degree of orientation.

Extrusion velocity influences the drawing process as follows: For a constant draw velocity and extrusion hole size, increases in extrusion rates decrease the differential between extrusion and draw velocities, decreasing the net drawing strain and therefore the amount of molecular orientation. If extrusion speeds are too slow, then sufficient material is not provided for drawing and fiber failure results. Therefore, extrusion rates should be just fast enough to continuously provide material at the exit hole. This corresponds to having a very small compressive load applied. For the slowest extrusion speed and high draw rates, the drawing phase actually begins inside the die. In this case, the fiber is drawn to a diameter smaller than the extrusion hole prior to reaching the exit point. The size of the extrusion hole then ceases to play a role in the deformation of the acrylic.

In summary, the finest, most highly oriented fibers are produced using a slow extrusion velocity, a small extrusion hole diameter to allow for the fastest draw rates, and a draw velocity as fast as the fiber will withstand without failure.

Quenching of the fibers into ice water virtually eliminates the drawing phase once the fiber has left the die. The fibers reach their glass transition temperature much more quickly, making drawing without breaking very difficult. The amount of deformation that was applied during drawing, as reflected by the fiber's diameter, though, had the same effect on molecular structure, whether the cooling temperature was 25 or 4°C. The fibers drawn through the ice water bath exhibited relaxation ratios of magnitudes similar to fibers of comparable diameter drawn through air, although producing those fibers was considerably more difficult.

### Molecular Deformation Mechanisms

To further examine the effects of orientation on the physical properties of these PMMA fibers, tensile tests of individual fibers were conducted. As previ-

ously discussed, extremely high ultimate tensile strengths and moduli were found for the most highly aligned fibers ( $\Gamma_L = 18.7$ ) and very high strains were seen in the fibers with the lowest degree of orientation ( $\Gamma_L = 6.0$ ). To gain some insight as to why these phenomena were observed, it is helpful to imagine the chains in the molten polymer prior to drawing to be similar to a loosely tangled mass of string. To a point, applied tensile deformation causes the stretching and alignment of the string, or the chains, but after a certain applied strain, the string that has not become aligned becomes so tightly tangled that further deformation is impossible; this is the point at which the fiber fails during drawing. Thus, the most highly aligned fibers drawn in this study can be considered to have relatively large areas of alignment and tightly tangled amorphous regions. In tension, then, the oriented regions exhibit the high tensile strengths observed, but the tightly tangled regions prohibit any further elongation, resulting in strains of only 3%, lower than for bulk acrylic. As less deformation is imposed during fiber formation (i.e., fiber diameter increases), oriented regions occupy less and less of the total fiber volume, and the amorphous regions become less tightly tangled. Therefore, ultimate tensile strength decreases, and elongation increases.

The thickest (0.0610 cm), least oriented fiber ( $\Gamma_L = 6.0$ ) whose true ultimate tensile strength was 78.0 MPa, and whose length increased during testing by 25% before failing, consists of oriented regions that are connected by loosely tangled amorphous regions, resulting in significant elongation with increased strength and modulus. The tensile strength, however, is limited by the relatively low degree of frozen-in alignment compared to the other fibers in this study.

The plots in Figures 10 and 11 depict only the behavior of partially oriented PMMA fibers. Extrapolation of these curves to  $\Gamma_L = 1$  should give the appropriate values of true stress and true strain for bulk acrylic. Figure 10 extrapolates to a value of about 20 MPa, which is a reasonable value for bulk acrylic. Examination of Figure 11, however, shows clearly that between  $\Gamma_L = 6$  and  $\Gamma_L = 1$ , strain must reach a maximum value and decrease to the bulk value of 5%. Although this behavior is not easily reconciled with simple models of molecular deformation, a scheme incorporating two competing mechanisms offers a more coherent explanation of the strain behavior observed in this study.

Tensile deformation of PMMA above its melt temperature can be thought to have two effects on the orientation of the molecular chains in the melt.



First, portions of chains in bundles aligned parallel or nearly parallel to the direction of deformation slide past one another, thereby increasing the total fraction of chains aligned along the fiber axis. Second, as a result of this chain sliding, portions of chains in amorphous regions become more tightly tangled, preventing them from sliding.

After the molecular structure imposed by the extrusion and drawing process has been frozen in, room temperature strain behavior is controlled by the amount of chain sliding permitted by the molecular structure in the fiber. At low relaxation ratios, chain sliding is controlled by the amount of orientation that was imposed during the formation of the fiber. In the bulk material there is little or no preferential orientation of chains in any direction, so that chain sliding is essentially prevented by steric hindrances of adjacent chains. As the amount of orientation along the fiber axis increases, chain sliding becomes increasingly easy, resulting in strain behavior following some increasing function as indicated by the dotted line in Figure 11. As the amount of imposed orientation continues to increase, however, chain sliding becomes hindered by the tightness of the entanglements in the amorphous regions and strain behavior follows a decreasing function as shown by the dashed line in Figure 11. Portions of chains that are aligned along the fiber axis and might otherwise slide easily past adjacent chains are prevented from doing so by the portions of the same chains that are restricted in tightly tangled amorphous regions. Although the fraction of chains aligned along the fiber direction is increasing in this region of the curve, resulting in the observed increasing tensile strength, these aligned chains are becoming increasingly immobile, resulting in the observed decrease in strain to failure.

Although the behavior of fiber ultimate tensile strength is straightforward for all degrees of orientation considered thus far ( $\Gamma_L = 1-19$ ), the question arises as to what theoretical maximum strength can be achieved by poly(methyl methacrylate). According to Griffith fracture theory, the tensile strength of a material,  $\sigma$ , is related to the size of the flaws present in the material such that

$$\sigma = (K/c)^{1/2}$$

where  $K$  is a constant encompassing Young's modulus, the energy required to form a flaw of critical size, and the shape of the sample and  $c$  is the flaw size. The theoretical maximum strength, then, is approached as the flaw size goes to zero. As discussed

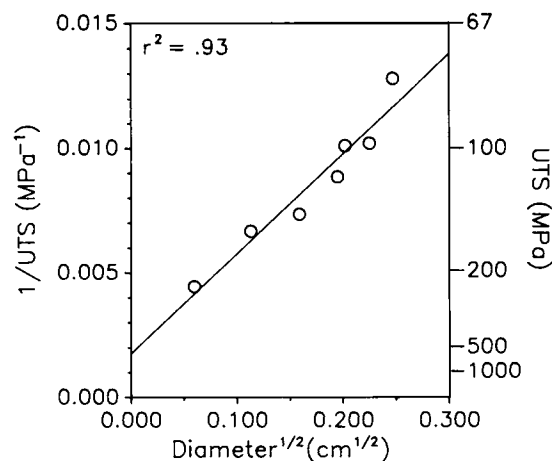


Figure 13 Theoretical maximum strength of acrylic fibers.

by Smook et al.,<sup>6</sup> for drawn fibers, this corresponds to a fiber whose diameter is approaching zero. According to the Griffith equation above, there exists a linear relationship between the reciprocal of ultimate tensile strength and the square root of the flaw size, or, here, the fiber diameter. Figure 13 illustrates this relationship for the seven different fiber types tested in this study. Extrapolation of this curve to zero diameter using linear regression with  $r^2 = 0.93$  ( $r = 0.96$ ) yields a theoretical maximum tensile strength of 570 MPa. Although the maximum strength observed in this study is five to ten times that of bulk acrylic, it is less than 40% of the theoretical maximum strength of poly(methyl methacrylate).

## CONCLUSIONS

1. Using a transient temperature drawing procedure, poly(methyl methacrylate) fibers were drawn into a range of diameters as small as 25  $\mu\text{m}$ . At the extrusion temperatures utilized, long polymer chains achieve sufficient mobility to be disentangled from neighboring chains and aligned in the direction of applied deformation.
2. The maximum draw ratio obtained in this study, measured by heat-induced relaxation, was on the order of 20. This is more than four times that previously reported.
3. Tensile strength was found to increase with increasing draw ratio to a maximum of 225 MPa for the fibers tested in this study. This

represents a sixfold increase over the strength of bulk acrylic.

4. PMMA fibers were found to exhibit true strains up to 25%, which is five times that observed in bulk acrylic. Strain to failure was observed to increase with increasing draw ratio at low draw ratios but to decrease with increasing draw ratio at all draw ratios above 6. Somewhere between draw ratios of 1 and 6, then, there exists a maximum strain to failure.
5. Young's modulus was found to increase with increasing draw ratio. The most highly aligned fiber tested here had a modulus of 7800 MPa, which is more than 10 times that of bulk acrylic.

## REFERENCES

1. B. M. Fishbane and S. R. Pond, *Clin. Orthop. Rel. Res.*, **128**, 194 (1977).
2. R. M. Pilliar and R. Blackwell, *J. Biomed. Mater. Res.*, **10**, 893 (1976).
3. S. Saha and S. Pal, *Trans. 7th Ann. Soc. Biomater.*, **4**, 21 (1981).
4. P. A. Botto, R. A. Duckett, and I. M. Ward, *Polymer*, **28**, 257 (1987).
5. I. M. Ward, *Structure and Properties of Oriented Polymers*, Wiley, New York, 1975, p. 13.
6. J. Smook, W. Hamersma, and A. J. Pennings, *J. Mater. Sci.*, **19**, 1359 (1984).

*Received February 26, 1991*

*Accepted May 14, 1991*